Improved Usability of a Low-Cost 5-DOF Haptic Device for Robotic Teleoperation

Gizem Ateş[1(✉)], Luca Brunetti[2], and Marcello Bonfè[2]

[1] Izmir Institute of Technology, Izmir, Turkey
gizemates@iyte.edu.tr
[2] Department of Engineering, University of Ferrara, Ferrara, Italy
luca.brunetti@student.unife.it,
marcello.bonfe@unife.it

Abstract. The paper describes the design and application of a low-cost haptic device with five degrees of freedom (5-DOF), all of which are fully actuated for force/torque haptic display. The device is realized using two Novint Falcons, commercially available haptic devices with only translational DOF. The paper focus on the practical issues related to the use of such a haptic device as a robotic teleoperation master and provides solutions to improve its usability during an application inspired by surgical robotics, namely the teleoperated insertion of a needle into a soft tissue. Experiments demonstrate the usefulness of force feedback and virtual fixtures on both translation and orientation degrees of freedom.

1 Introduction

In robotic teleoperation, a key role is played by the master device interacting with humans, providing motion commands to a slave manipulator and returning haptic (i.e. force/torque) feedback [1]. Desired features of such haptic devices are back drivability, smoothness of motions and accuracy of force/torque display [2, 3].

On the other hand, mechanical devices with such features and providing haptic feedback on more than 3 DOF are commonly quite expensive. As an example, the 3D Systems *TouchTM* can move in 6-DOF but display only translational forces[1]. The Force Dimension *delta.6* is a full 6-DOF haptic device, but costs about ten times more than a *TouchTM* device. The one used in this study is Novint Falcon's 3-DOF haptic device which is a desktop scale kind of Delta robot, a parallel manipulator with only translational DOF first described in [4].

Inspired by the work of Shah et al. (2010) [5] at the Utah University Telerobotics lab, we assembled a 5-DOF haptic device[2], with minor modifications to the original mechanical design, but a large rework of the kinematics and force/torque display, focused on control software implementation for robotic teleoperation. Next sections will describe first the mechanical features of this 5-DOF system and then how the issues related to its practical use in robotics have been addressed. Furthermore, some

[1] https://www.3dsystems.com/haptics-devices/touch.
[2] http://www.forcedimension.com/products/delta-6/overview.

V. Arakelian and P. Wenger (Eds.): *ROMANSY 22 - Robot Design, Dynamics and Control*, pp. 213–221, 2019.
https://doi.org/10.1007/978-3-319-78963-7_28

mechanical limitations have been mentioned and solutions offered. In the final chapter, experimental results discussed under both master/slave coupled and non-coupled teleoperation schemes.

2 Mechanical Design of the 5-DOF Haptic Device

The Novint Falcon is a 3-DOF haptic device allowing only translational motions, while rotational motions are constrained. Indeed, the kinematic structure of the Falcon is derived from the Delta type of parallel manipulators, whose so-called moving platform, generally assumed as the end-effector for manipulation, has a fixed orientation thanks to parallelograms mechanisms. The Novint Falcon's representative axes of motion, associated to the moving platform, are shown in Fig. 1.

Fig. 1. Coordinates convention of the original Novint Falcon

Connecting the end-effectors of two 3-DOF Falcon devices, by means of a rigid link and two spherical joints, allows to create a 5-DOF device. A first issue to address in the design of this connection is to obtain the largest possible work-space. The workspace features of Falcon are thoroughly investigated in [6]. By considering this study, each Falcons' gravity compensated origin positions, where a single Falcon reaches its largest workspace, were chosen the initial states. Then, workspaces of two Falcons have been overlapped assuming that one of the two should be rotated along the Z-axis by 90°. Therefore, each Falcons' end effectors have the same (X, Y) coordinates whereas there is an offset in between them along Z axis, as the length of the stylus plus screw depth. The center of this intersection was then taken as the workspace origin. Excluding spherical joints that were replaced by commercially available equivalents, the placements of Falcons in initial state can be described as shown in Fig. 2.

The work of Shah et al. introduces specifically designed extensions, to be mounted replacing part of the original Falcon grip, allowing to move the tip of the end effector along the X and Z directions. These extensions do not affect the previously described

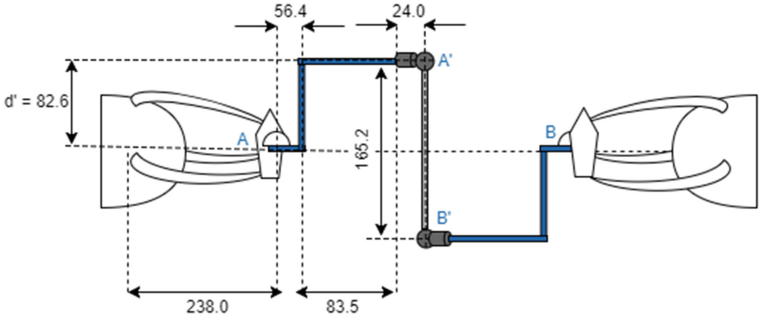

Fig. 2. Dimensions of connector parts from side view (in millimeters)

workspace optimization, but require to adapt accordingly the fixture of the Falcon bases. Considering the same dimensions for most the end-effector extending parts used in Shah et al. excluding spherical joints that were replaced by commercially available equivalents, the placements of Falcons in initial state can be described as shown in Fig. 2.

The total distance from one Falcon's origin to the stylus middle point is calculated as 401.9 mm. As a consequence, relative placements of Falcons is designed as in Fig. 3.

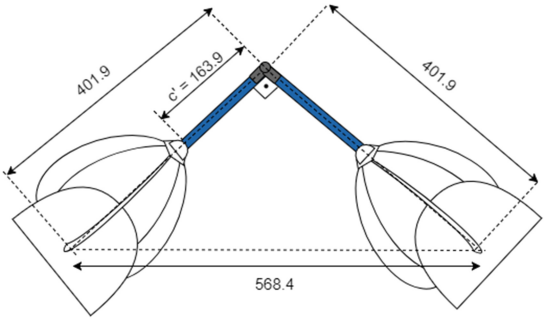

Fig. 3. Placements of each Falcon devices with respect to each other

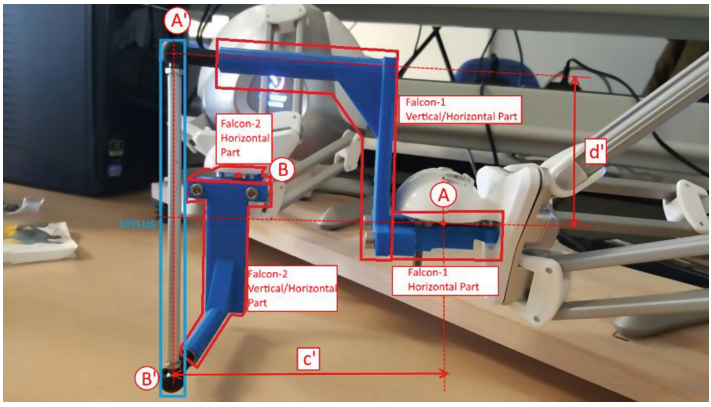

Fig. 4. Final design of the new 5-DoF device

The final model was assembled as shown in Fig. 4. Parts named as "Horizontal Part" and "Vertical/Horizontal Part" were printed by using *MakerBot 3D printer*. On the other hand, stylus is an aluminum stick with length 141.3 mm. Adding up the screw offsets and the distance between A′ and B′ was evaluated as 165.2 mm.

3 Kinematics and Force/Torque Display

The kinematics of the Novint Falcon is well known, being equivalent to the general Delta robot. Therefore, only the position and orientation of the stylus is considered in this section. For ease of calculations, it is assumed that one Falcon's body frame is coincident with the world frame. Therefore, the second Falcon's body frame is obtained by rotating it 90° around the Z-axis according to the first Falcon's body frame.

Known variables are the end effector positions of each Falcon with respect to their own body frame. The point A at initial state is assumed to be the origin of the system. Hence point B at initial state is calculated as follows,

$$\overrightarrow{B} = d'(\overrightarrow{x_1}\cos(\frac{\pi}{4}) - \overrightarrow{y_1}\sin(\frac{\pi}{4}))$$

where d' is the initial distance of point A′ to the middle point of stylus (see Fig. 2), while $\overrightarrow{x_1}$ and $\overrightarrow{y_1}$ are the unit vectors of the first Falcon device's body frame.

In order to evaluate the position of the new 5-DoF haptic device, the middle point position of stylus and for the orientation, A' and B' points are used. Hence the state of the end effector of the 5-DOF device becomes a line equation whose one specific point and slope are known.

The orientation of the stylus is calculated as follows:

$$\langle x_{A'}, y_{A'}, z_{A'}\rangle = (x_A + c')\overrightarrow{x_1} + y_A\overrightarrow{y_1} + (z_A + d')\overrightarrow{z_1}$$

$$\langle x_{B'}, y_{B'}, z_{B'}\rangle = \overrightarrow{B} + (x_B + c')C^{(1,2)}\overrightarrow{x_2} + y_BC^{(1,2)}\overrightarrow{y_2} + (z_B + d')C^{(1,2)}\overrightarrow{z_2}$$

The middle point of the stylus is calculated from the general line equation

$$\langle x, y, z\rangle = \langle x_{A'}, y_{A'}, z_{A'}\rangle + d'\langle m_x, m_y, m_z\rangle$$

where $\langle m_x, m_y, m_z\rangle$ is the slope of the line calculated as

$$\langle m_x, m_y, m_z\rangle = \langle x_{A'}, y_{A'}, z_{A'}\rangle - \langle x_{B'}, y_{B'}, z_{B'}\rangle$$

Finally, force and torque to be displayed at the stylus of the 5-DOF haptic device can be theoretically calculated with vector operations similar to those described by Shah et al. (2010). However, from the practical point of view the perceived quality of such a force/torque display is strongly affected by the mechanical properties of the spherical joints of the Falcons that tends to get stuck when the device is moved near the workspace limits. Moreover, the workspace itself is further reduced compared to the one of an isolated Falcon. Next section will describe proposed solutions for virtual workspace augmentation and for improving the 5-DOF haptic feedback.

4 Workspace Scaling and Virtual Constraints

The most common solution to match the workspaces of master and slave devices in robotic teleoperation is to scale the motion of one of the two. Purely translational motions can be simply multiplied by a desired scaling factor, while rotational motions, that turned out to be quite limited in the device (i.e. 26° maximum angle of the stylus from the initial vertical position), must be handled with different mathematical tools. If quaternions are used to describe 3D orientations, it is possible to define a consistent equivalent to the translation scaling in terms of quaternion power operation. Indeed, while successive translational motions simply sum up, successive rotations expressed as quaternions are multiplied, using the quaternion multiplication. Equivalently, scaling a quaternion q by a factor k translates into q^k (see reference [7]). More generally, scaling a quaternion q relatively to an initial reference q_0 can be implemented as follows:

$$q_s = (qq_0^{-1})^k q_0$$

Notice the previous formula is essentially the so-called SLERP (Spherical Linear intERPolation, see reference [8]), here used to extrapolate an orientation along the arc connecting two quaternions, rather than interpolate between the two quaternions. For the considered 5-DOF device, two different choices of the scaling factor were tested: a constant value of 2 and a nonlinear function of the angle with respect to the initial orientation q_0, as suggested by [7]. However, the latter was judged cumbersome by most of the users involved in the experiments.

Another issue related to the limitations of the original Novint Falcon, is due to the fact that in some positions, close to the workspace limits and in which the spherical joints of the device arms get stuck, the user needs to apply more force than he/she would apply to move the grip in free space. In practice, the user feels an unintended haptic feedback that of course disrupts the transparency of the desired force/torque display.

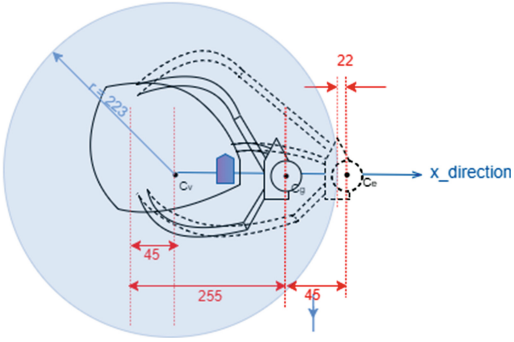

Fig. 5. Virtual constraint

In order to prevent the end effector of each Falcon device to reach this critical point, a virtual spherical constraint was designed as shown in Fig. 5. The drawing shows two positions of the Falcon device surrounded by the virtual constraint. One representation shows the initial position of Falcon device (i.e. in the middle point of its workspace). Tip point of this position is labeled as Cg. Second representation shows the position reaching the upper bound in X-direction. Tip point of this position is labeled as Ce. The virtual constraint is implemented in software as a surface with a high stiffness, providing a repulsive force

directed along the normal to the surface and towards the center of the sphere. This force is summed to the one calculated from force/torque display of the 5-DOF haptic interface, but is actually perceived by the user as a mechanical end-stop. By designing this virtual constraint so that the real mechanical limits of the device are never reached and, therefore, its joints don't get stuck, the user receives a more intuitive and transparent haptic feedback.

After practical experiments, the virtual constraints has been modeled as a sphere with a 223 mm radius, whose center is 210 mm from the workspace center in the negative X-direction. The stiffness of the surface of the sphere was chosen as 1000 N/m.

5 Control Architecture for Robotic Teleoperation

Two different teleoperation schemes were implemented and tested. In the first scheme, shown in Fig. 6, the slave manipulator tracks the reference pose x_c calculated by an admittance controller, receiving as inputs the measurement of a force/torque sensor mounted on the robot tip and the reference pose x_m generated by the haptic master, after scaling. The admittance controller is governed by the following mathematical model:

$$M\ddot{x}_c + B\dot{x}_c + K(x_c - x_m) = F_{in}$$

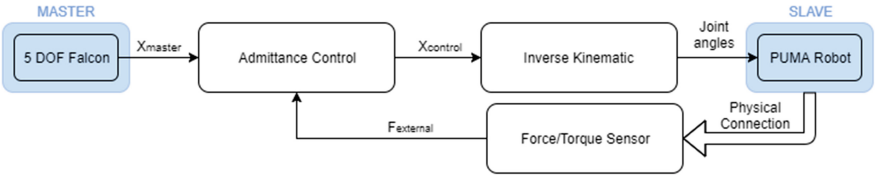

Fig. 6. Control diagram without coupling between master and slave

In the second scheme, shown in Fig. 7, besides admittance control there is a spring/damper coupling between master and slave, generating a force that is used on one side as the haptic force to be displayed and on the other side as an input for the admittance controller, to be summed at the external force measured by the sensor at robot tip. The coupling block is therefore governed by the following law:

$$F_{master} = K_c x_e + B_c v_e$$

where x_e and v_e are the position and velocity errors defined as: $x_e = x_{master} - x_{slave}$, $v_e = \dot{x}_{master} - \dot{x}_{slave}$

The force applied to the slave is: $F_{slave} = -F_{master}$

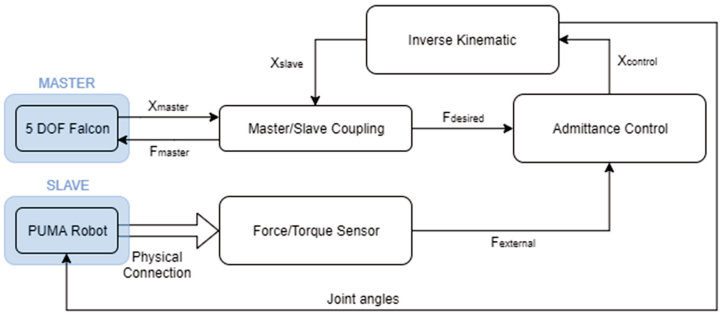

Fig. 7. Control diagram with coupling between master and slave

6 Teleoperation Task and Experiments

In experimental procedure a 6-DoF PUMA 260 robotic arm is used. The pose of the robot is teleoperated by means of the 5-DOF haptic device, applying as an additional constraint on the tool orientation the previously described choice of the full 3D orientation of the haptic stylus.

The proposed experiment consists of the emulation of a surgical needle insertion into a soft tissue. Our tissue model is a two-layered artificial phantom whose upper layer is artificial skin and lower layer is a soft non-fluid wax, mimicking natural tissue with both skin and ligament. Before the needle is fully inserted into the skin, the artificial skin applies more reflected force. As soon as the skin is worn through, the reflected force decreases because of the lower stiffness of wax simulating the ligament.

Table 1 shows the chosen constants to design controller/and coupler. Moreover, Figs. 8 and 9 shows the position vs. force measurements respectively according to these constants.

Table 1. Constants to design controller/and coupler

<Force, Moment>	Without Master/Slave Coupling (Fig. 8)	With Master/Slave Coupling (Fig. 9)
Coupling damping	-	<5.0, 1.2>
Coupling stiffness	-	<170.0, 4.0>
Controller damping	<30.0, 1.2>	<30.0, 1.2>
Controller stiffness	<160.0, 5.0>	<160.0, 5.0>

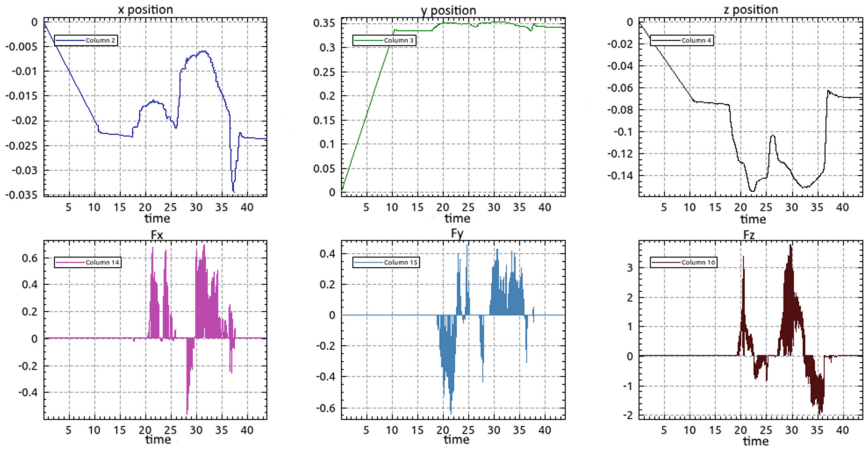

Fig. 8. Experimental results in non-coupled teleoperation scheme with two penetrations

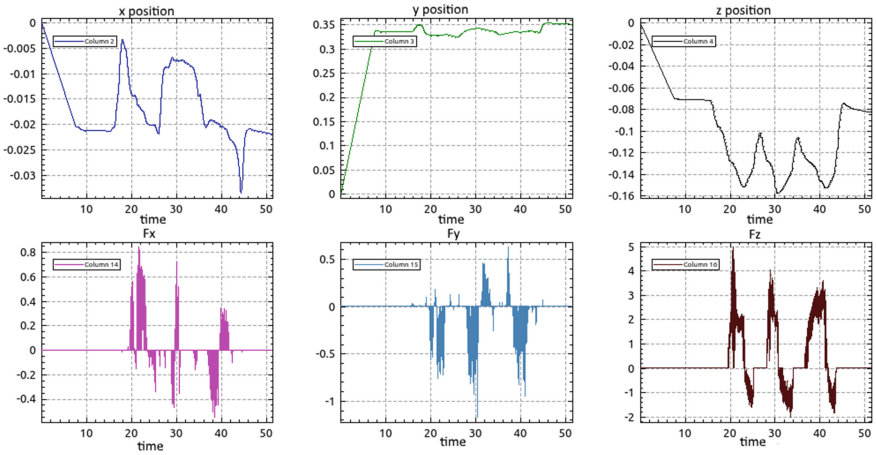

Fig. 9. Experimental results in non-coupled teleoperation scheme with three penetrations

7 Conclusion and Future Work

In this study, we elaborate a low cost 5-DoF haptic device inspired by Shah et al. (2010). In addition to building it, we improved its workspace and reduced its position level singularity problems by adding a virtual wall. Moreover, we used this new 5-DoF device in a teleoperated needle insertion scenario. The experimental results verified the effectiveness of the haptic device with various control parameters in free motion and simultaneous position and force changing scenario.

Despite the need to optimize controlling parameters for specific task, the device is more than sufficient to be used as a master 5-DOF device in teleoperated haptic applications.

References

1. Okamura, A.M.: Haptic feedback in robot-assisted minimally invasive surgery. Curr. Opin. Urol. **19**(1), 102–107 (2009)
2. Zinn, M., Khatib, O., Roth, B., Salisbury, J.K.: Playing it safe. IEEE Robot. Autom. Mag. **11** (2), 12–21 (2004)
3. Hayward, V., et al.: Haptic interfaces and devices. Sens. Rev. **24**(1), 16–29 (2004)
4. Clavel, R.: Conception d'un robot parallèle rapide à 4 degrés de liberté, EPFL, Lausanne, Switzerland (1991)
5. Shah A.V., Teuscher S., McClain E.W., Abbott J.J.: How to build an inexpensive 5-DOF haptic device using two Novint Falcons. In: Lecture Notes in Computer Science (including Subseries Lecture Notes in Artificial Intelligence, Lecture Notes in Bioinformatics). LNCS, vol. 6191, part 1, pp. 136–143 (2010)
6. Martin, S., Hillier, N.: Characterisation of the Novint Falcon haptic device for application as a robot manipulator. In: Australasian Conference on Robotics and Automation (ACRA), pp. 1–9 (2009)
7. Poupyrev I., Weghorst S., Otsuka T., Ichikawa T.: Amplifying spatial rotations in 3D interfaces. In: CHI 1999 Extended Abstracts on Human Factors in Computing Systems, p. 256 (1999)
8. Shoemake, K.: Animating rotation with quaternion curves. ACM SIGGRAPH Comput. Graph. **19**(3), 245–254 (1985)